Application of infrared light for *in vivo* neural stimulation

Jonathon Wells
Vanderbilt University
Department of Biomedical Engineering
Box 351631, Station B
Nashville, Tennessee 37235

Chris Kao
Vanderbilt University
Department of Neurological Surgery
1161 21st Avenue
Nashville, Tennessee 37235

E. Duco Jansen
Peter Konrad
Anita Mahadevan-Jansen
Vanderbilt University
Department of Biomedical Engineering
Box 351631, Station B
Nashville, Tennessee 37235
    and
Vanderbilt University
Department of Neurological Surgery
1161 21st Avenue
Nashville, Tennessee 37235

Abstract. A novel method for damage-free, artifact-free stimulation of neural tissue using pulsed, low-energy infrared laser light is presented. Optical stimulation elicits compound nerve and muscle potentials similar to responses obtained with conventional electrical neural stimulation in a rat sciatic nerve model. Stimulation and damage thresholds were determined as a function of wavelength using a tunable free electron laser source ($\lambda = 2$ to 10 μm) and a solid state holmium:YAG laser ($\lambda = 2.12$ μm). Threshold radiant exposure required for stimulation varies with wavelength from 0.312 J/cm^2 ($\lambda = 3$ μm) to 1.22 J/cm^2 ($\lambda = 2.1$ μm). Histological analysis indicates no discernable thermal damage with suprathreshold stimulation. The largest damage/stimulation threshold ratios (>6) were at wavelengths corresponding to valleys in the IR spectrum of soft tissue absorption (4 and 2.1 μm). Furthermore, optical stimulation can be used to generate a spatially selective response in small fascicles of the sciatic nerve that has significant advantages (e.g., noncontact, spatial resolution, lack of stimulation artifact) over conventional electrical methods in diagnostic and therapeutic procedures in neuroscience, neurology, and neurosurgery. © *2005 Society of Photo-Optical Instrumentation Engineers.* [DOI: 10.1117/1.2121772]

Keywords: optical stimulation; peripheral nerve stimulation; lasers; neural excitation techniques.

1 Introduction

Neural stimulation is the process of initiating action potentials in peripheral and central neurons through an external energy source. Initiation of action potentials is an important intervention in many research and clinical procedures as a therapeutic or diagnostic tool. The excitation of neural tissue also has numerous applications in basic science and is a valuable tool for the research community. Despite the clinical and research relevance of neural activation, there has been little progress in the basic method and implementation used for this purpose. Here we discuss the emergence of a novel method for neural stimulation using pulsed infrared light that takes advantage of the unique properties and selectivity of optics in a fundamental technique ubiquitous in all areas of neuroscience, namely stimulation. We define optical stimulation as applied incident light acting on neural tissue causing a transient energy deposition in that tissue directly resulting in an evoked action potential (AP).

Whether studying single cells or modifying nerve cell function in humans during clinical procedures, the traditional history of neuronal or nerve stimulation is based on electrical methods. Since the 1800s, use of transient electrical stimulation continues as the primary methodology to initiate APs in

neurons to date.[1–5] The main advantages of electrical stimulation include ease by which (1) stimulation parameters can be controlled and quantified (intensity, duration, frequency) and (2) electrodes can be manufactured.

However, electrical stimulation of individual neurons is constrained by the need to (a) use microelectrodes to target specific cells, which are incompatible with long term implantation in animals or humans, and (b) separate the desired information from electrical background noise.[6–9] Existence of an electrical stimulation artifact has plagued electrophysiologists for decades by making simultaneous stimulation and recording from adjacent portions of the neuron difficult[10] without the use of complicated systems employing modified forward-masking techniques.[11] Most extracellular electrodes stimulate not only neurons immediately adjacent to the electrode but also many other neurons surrounding the region in a spatially decaying fashion. To selectively stimulate an individual neuron, the electrode must be typically very close to the neuron or impale the neuron (intracellular electrode). Electrical stimulation methodology therefore lacks the spatial specificity needed to target individual sensory or motor fibers in the central and peripheral nervous systems without physically invading the immediate region surrounding the neuron. Regardless, all applications that presently attempt neural activation are primarily based on electrical methods. In summary, the limitations of electrical stimulation include high-

Address all correspondence to: Anita Mahadevan-Jansen, PhD, Vanderbilt University, 5803 Stevenson Center, 2201 West End Avenue, Nashville, Tennessee 37235. Tel: 615-343-4787. Fax: 615-343-7919. E-mail: Anita.Mahadevan-Jansen@vanderbilt.edu

frequency artifacts associated with the stimulation signal that limit data analysis and prevent simultaneous stimulation and recording of adjacent areas, tissue damage by the placement of the electrode in close proximity to neurons, a population response due to the recruitment of multiple axons, and, in general, poor spatial specificity.

Although the gold standard of neural stimulation is by electrical means, it is well known that action potentials can be triggered in neurons using many different stimuli including electrical, mechanical, magnetic, thermal, and chemical means. Conventionally, the initiation and propagation of action potentials within neurons have been explained with electrical stimulation on the basis of a transmembrane ionic exchange, in which the induction of explosive opening of sodium channels occurs when the transmembrane voltage potential is increased to a threshold value (typically about −50 mV). An alternative interpretation for the activation of neurons suggests that small amounts of free energy are required for the repeated induction of action potentials.[12] This energy may come in the form of chemical reactions. For instance, changing the concentration of ions surrounding nerve cells *in vitro*[13] can lead to external stimulation; however, these methods are not practical for *in vivo* applicability, such as in the clinical setting. There have been several reports on the excitability of neural tissue as a by-product of laser therapies and the capability of light in modulating its electrical conductivity.[14–21] Optical stimulation of a bundle of central nervous system fibers was reported by Allegre et al. using a short-pulse ultraviolet excimer laser[22]; however, energies required for stimulation were at the tissue damage threshold. More recently, the activation of cultured neurons was reported using multiphoton excitation with a femtosecond laser.[23] However, Wells et al. have reported on the simple concept of using pulsed, low-level infrared light to elicit nerve action potentials and its clinical utility.[24]

Lasers and light, in fact, are widely and successfully used in a number of clinical procedures. Classically, the biological applications of lasers have been in high-energy effects such as tissue thermal degradation[25,26] and ablation.[27,28] However, because of the advantages of narrow linewidth with appreciable energy, as well as the inherent benefits such as coherence and monochromaticity, a variety of low-power laser applications have emerged. Alternatively, lasers have been used for a variety of applications known as biostimulation or low-level light therapy (LLLT). In this modality, low fluence levels at laser wavelengths that are weakly absorbed in tissue are applied continuously for a prolonged duration to improve wound healing, stimulate hair growth, alter pain perception, etc. Due to largely unknown mechanisms, the laser radiation modulates biological processes such as inflammation, cell proliferation, cytokine release, etc. On the other hand, optical stimulation of neural tissue is the transient deposition of energy leading to activation of a potential as a direct result of incident light. This methodology used radiant exposures at wavelengths that are more strongly absorbed than in LLLT. Nevertheless, we have demonstrated the radiant exposure needed to induce neural stimulation is well below the threshold for inducing permanent damage to the tissue.[24] We will refer to the radiant exposure needed for optical stimulation of neural tissue as "low level" relative to the conventional therapeutic laser applications that lead to tissue coagulation and ablation.

This paper aims to provide evidence that optical energy from a pulsed laser provides the free energy transition necessary to activate neural tissue. We systematically prove that low-level laser stimulation of nerves does not include many of the inherent concomitant impediments of electrical stimulation. Results present evidence demonstrating that laser excitation of neural activity provides a contact-free, spatially selective, artifact-free method of stimulation without incurring tissue damage that may have significant advantages over electrical methods for many diagnostic and therapeutic clinical applications. The primary goals of this paper are to assess the physiologic validity of optical stimulation in the sciatic nerve in rats, characterize the wavelength dependence of this phenomenon, and determine the safety therefore damage induced by this modality.

2 Methods

All experiments were conducted at the Vanderbilt University W.M. Keck Free Electron Laser Center and Vanderbilt Biomedical Optics Laboratory following approval by the Institutional Animal Care and Use Committee (Protocol M/01/115).

2.1 Nerve Preparation

In vivo sciatic nerve experiments were performed using Spraque-Dawley rats (300 to 350 g). Rats were anesthetized through intraperitoneal injection of ketamine (80 mg/kg) and xylazine (10 mg/kg) solution and maintained sedated for the duration of each individual experiment with 30 mg ketamine every 30 min. Nerve preparation consisted of shaving the skin over the thigh and aseptically prepping the area with betadine. An incision was then made in the thigh exposing the main trunk of the sciatic nerve from the ischeum to the knee. Muscular fascia was incised and removed to expose the nerve, and the epineurial (outer) covering of the nerve was left intact.

2.2 Electrical Stimulation and Recording Technique

Electrical stimulation and recording was first performed in each experiment for comparison with the optical stimulation response using a classic preparation most neurophysiologists are familiar with, namely the rat sciatic nerve preparation.[29] Muscle potential and visible muscle contraction were used to qualitatively and quantitatively assess the effectiveness and impact of optical stimulation relative to electrical stimulation, which served as the gold standard for all experiments. At the beginning of every stimulation experiment, the sciatic nerve was electrically stimulated (electrical parameters ranged from 0.3 to 0.6 V; 5-μs pulse duration; single pulse frequency) in a branch of the nerve known to innervate the hamstring muscle (Fig. 1). Usually the electrode was located proximal to the first branch point of the sciatic nerve. A compound nerve action potential (CNAP) was recorded using silver chloride electrodes (Grass needle electrode) in contact with the nerve located typically 15 mm from the stimulation point. Additionally, a compound muscle action potential (CMAP) was recorded using the same type of stainless steel needle electrodes pierced into the hamstring muscle (Fig. 1). The distance was measured (in millimeters) between the cathodal stimulating electrode and the recording electrodes to facilitate measurement of CNAP conduction velocities (m/s).
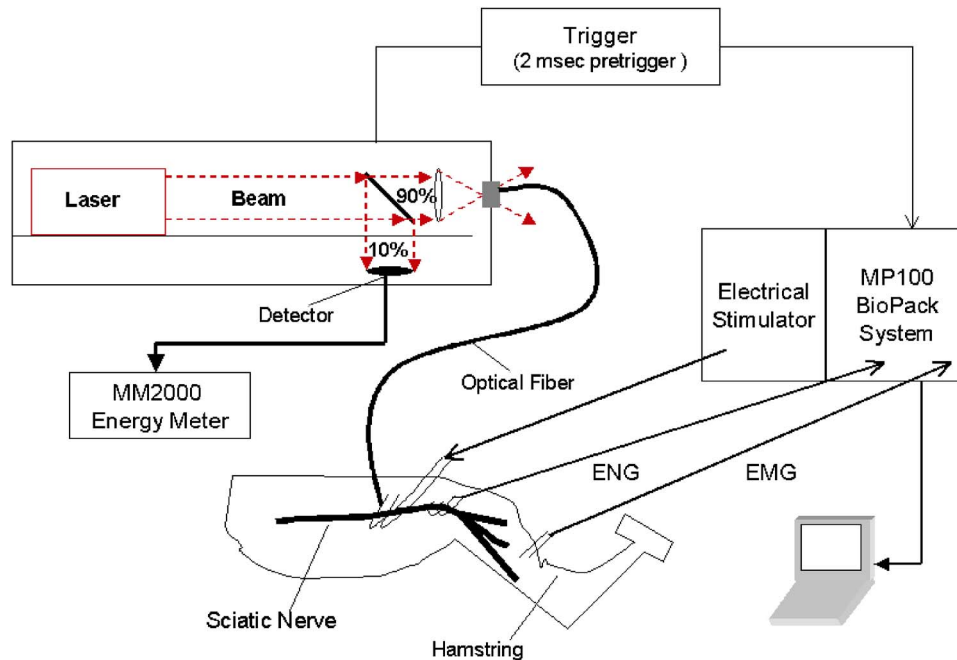
Fig. 1 Schematic of the experimental setup used in all experiments. The laser used was a fiber-coupled holmium:YAG laser (shown), or in some cases the FEL applied through a hollow waveguide was used to stimulate the peripheral nerve proximal to the first branch point.

CNAP and CMAP responses to optically and electrically stimulated nerves were recorded with a modular data acquisition system (MP100, Biopac Systems Inc., Santa Barbara, CA) controlled using a computer and the Acknowledge software (Biopac Systems Inc.). CNAP and CMAP recordings were pretriggered 2 ms prior to stimulation of the nerve and ended 30 ms later, when the response was clearly over. An amplification of $1000\times$ was applied, and all signals were filtered with a bandpass filter of 50 to 500 Hz.

2.3 Optical Stimulation

Two infrared laser sources were used to stimulate the nerves optically. A free-electron laser (FEL),[30–33] tunable from 2 to 10 μm, was initially used to assess the optimal IR wavelengths for optical activation. The unique pulse structure of the Vanderbilt FEL incorporates a train of 1-ps energy spikes, called micropulses, at a repetition rate of 3 GHz. The envelope of this pulse train forms a 5-μs macropulse that can be delivered at a repetition rate varying from 1 to 30 Hz. The free beam is deflected onto the optical table where the experiment is performed and focused using a CaF$_2$ lens (biconvex lens, $f=200$ mm) into a 500-μm-diameter hollow waveguide[34] positioned 0.75 mm above the exposed sciatic nerve (spot size=0.6 mm^2) to initiate action potential propagation. A double Brewster plate polarizer is used to vary the laser pulse energy, measured using a Molectron laser energy meter (MM2000 with LP50 head) set to calculate an average energy per 10 pulses. Six wavelengths at or near relative peaks and valleys in infrared water absorption, 2.1, 3.0, 4.0, 4.5, 5.0, and 6.1 μm, at a repetition rate of 2 Hz were used for this study.

Using the results from the FEL study, a portable holmium:YAG laser (1-2-3 laser, Schwartz Electro Optics, Inc.) was used to further evaluate optical laser stimulation at an identi-

fied optimal infrared wavelength. Using a CaF$_2$ lens with a focal length of 25 mm, the holmium:YAG laser beam is coupled into a 600-μm-core optical fiber (NA=0.39±0.02) and distally delivered to the nerve. The fiber-to-nerve distance was held constant at 0.75 mm yielding a spot size of 1.198 mm^2. This laser operates at a wavelength of 2.12 μm with pulse duration of 250 μs (FWHM). The radiant exposure used to stimulate is roughly 0.3 to 0.7 J/cm^2, at a repetition rate of 2 Hz. To account for pulse-to-pulse instability in the laser output, a beamsplitter is used to pick off and measure 10% of the energy delivered for each pulse. A correlation factor between the measured energy and the energy delivered to the tissue was calculated before each set of experiments to determine the energy of each individual pulse.

2.4 Fourier Transform Infrared (FTIR) Spectroscopy of Rat Sciatic Nerve Tissue

The purpose of this study was to determine the tissue absorption characteristics for the rat sciatic nerve over a range of wavelengths within the infrared spectrum using a FTIR spectrometer. This information was evaluated to identify appropriate wavelength(s) for optical stimulation of the nerve fibers while causing minimal damage to the tissue. Rat sciatic nerve tissues from three rats (six nerves) were extracted. Sciatic nerve sections spanning from the spinal cord to the first major branch point, approximately 2.5 cm in length, were removed while under anesthesia or shortly after euthanasia. Upon extraction, the nerves were immediately transferred into a sealed tube and frozen with liquid nitrogen. Tubes were then placed in a $-70°$C freezer until data collection began. Nerves were thawed using a saline solution mimicking extracellular fluid that normally bathes the nerve. To obtain reliable optical property measurements the nerve was finely minced, or liquefied.[35] This served to (1) maintain consistency in the

sample and eliminate air bubbles for accurate data collection, and (2) permit measurement from a sufficiently thin layer of tissue sample for transmission mode in the FTIR setup.

A FTIR spectrometer (Bruker IRS 66V) in transmission mode, equipped with a globar source and DTGS detector, was used to determine the IR absorption of rat sciatic nerve tissue preparations as a function of wavelength from 2 to 6.1 μm. The spectrometer was purged with nitrogen gas to facilitate transmission of the IR beam and the laser was set to 32 scans per acquisition at a resolution of 4 cm^{-1}. Data was sent to OPUS® software for data analysis, while a baseline measurement of pure water was used as the reference material. This procedure provided the absorption coefficient as a function of wavelength from 2 to 6.1 μm.

2.5 *Wavelength Dependence and Safety Ratio Measurement*

Studies to discern general trends in the relationship between stimulation thresholds as a function of the infrared absorption spectrum were conducted to evaluate the optimal wavelength for safe, efficient laser excitation of neural tissue. Stimulation threshold is defined as the minimum radiant exposure required for a visible muscle contraction occurring with each laser pulse. Ablation threshold is defined as the minimum radiant exposure required for visible cavitation or ejection of material from the nerve, observed using an operating microscope, with 10 laser pulses delivered at 2 Hz. For threshold studies, optical stimulation was performed at different wavelengths (λ =2.1, 3.0, 4.0, 4.5, 5.0, and 6.1 μm) lying on relative peaks or valleys in the infrared spectrum based on FTIR measurements using the FEL at a repetition rate of 2 Hz with radiant exposures ranging from 0.3 J/cm^2 to just above 1.0 J/cm^2 for stimulation threshold and 0.3 J/cm^2 to over 6.0 J/cm^2 for ablation threshold. Within the possible operating range of the FEL (1 to 30 Hz), this repetition rate was chosen to aid recording and analysis of a visible twitch and APs. The ablation threshold varies across the infrared spectrum owing to the wavelength dependence of the absorption coefficient. Therefore, a more useful indicator of optimal wavelength for laser stimulation is the ratio of the radiant exposure for the threshold of ablation versus muscle contraction for a given wavelength. This ratio identifies spectral regions with a large margin between radiant exposures required for excitation and damage.

2.6 *Histological Analysis of Irradiated Peripheral Nerve*

Histological analysis was performed to assess the damage to the tissue from optical stimulation. For this acute damage study, the sciatic nerve was harvested immediately following laser irradiation at two different sites along a smaller nerve branch, distal to the first division of the main sciatic nerve. The neural tissue was irradiated with 10 laser pulses *in vivo* at a particular energy slightly above stimulation threshold with the FEL. A control lesion was placed on a different portion of the nerve with 20 laser pulses, approximately 3 to 5 mm from the experimental spot, with energies near the tissue ablation threshold at that wavelength. Radiant exposure was varied for a total of 12 irradiated nerves comprising four wavelengths; namely, 4, 4.4, 5, and 5.4 μm. Lower radiant exposures as

Table 1 Four-point grading scheme employed by neuropathologist and laser-tissue interaction expert to quantify the extent of damage accrued as a result of laser irradiation of the nerve.

Grade	Associated changes to the tissue
0	No visible thermal changes
1	Thermal changes in perineurium, no nerve damage
2	Thermal damage in perineurium extending to the interface of the perineurium and the nerve
3	Thermal damage in perineurium and in nerve

compared to experiments reported above were used to stimulate the smaller nerve branch (range: 0.135 to 5.85 J/cm^2), due to the lower stimulation threshold at this site (average: 0.14 J/cm^2). After each experiment, the sciatic nerve was marked with methylene blue where optical stimulation was incident on the nerve, while control lesions were marked with black India ink. The nerve was then extracted, immediately placed in formalin, and prepared into slides of 5-μm-thin longitudinal sections. Areas of coagulation, axonal disruption, and perineurium damage were assessed using light microscopy and routine hematoxylin and eosin (H & E) staining. The excised nerves were sent for an independent review of histological changes that occur with laser stimulation and ablation (Fig. 3), interpreted by an expert in histopathology associated with laser-tissue interaction.[36] Changes sought in laser irradiated tissue include: (1) collagen hyalinization, (2) collagen swelling, (3) coagulated collagen, (4) decrease or loss of birefringence image intensity, (5) spindling of cells in perineurium and in nerves (thermal coagulation of cytoskeleton), (6) disruption and vacuolization of myelin sheaths of nerves, (7) disruption of axons, and (8) ablation crater formation.[37] These criteria help define a four-point grading scheme assigned to each specimen indicating extent of damage at the site of optical stimulation (Table 1).

3 Results

3.1 *Physiologic Validity of Measured Signal*

Proof of concept studies were initially performed *in vivo* on the sciatic nerve of a rat where neural activity was stimulated using a pulsed infrared laser source, compared with electrical stimulation. Subsequent CNAPs and CMAPs were recorded using conventional electrical recordings (Fig. 2). Potentials from both nerve and muscle from each of the stimulation modalities are compared in Fig. 2. Recordings reveal very little difference between optical and electrical stimulation in both the nerve and muscle. It is clear that the shape and timing of these responses are similar. Therefore the conduction velocities are comparable between axons that are recruited with either stimulation modality. Furthermore, it is apparent from Figs. 2(a) and 2(c) that the stimulation artifact present in electrical stimulation recordings (t=0) is not observed with optical stimulation. As incident energy (J/cm^2) was in-
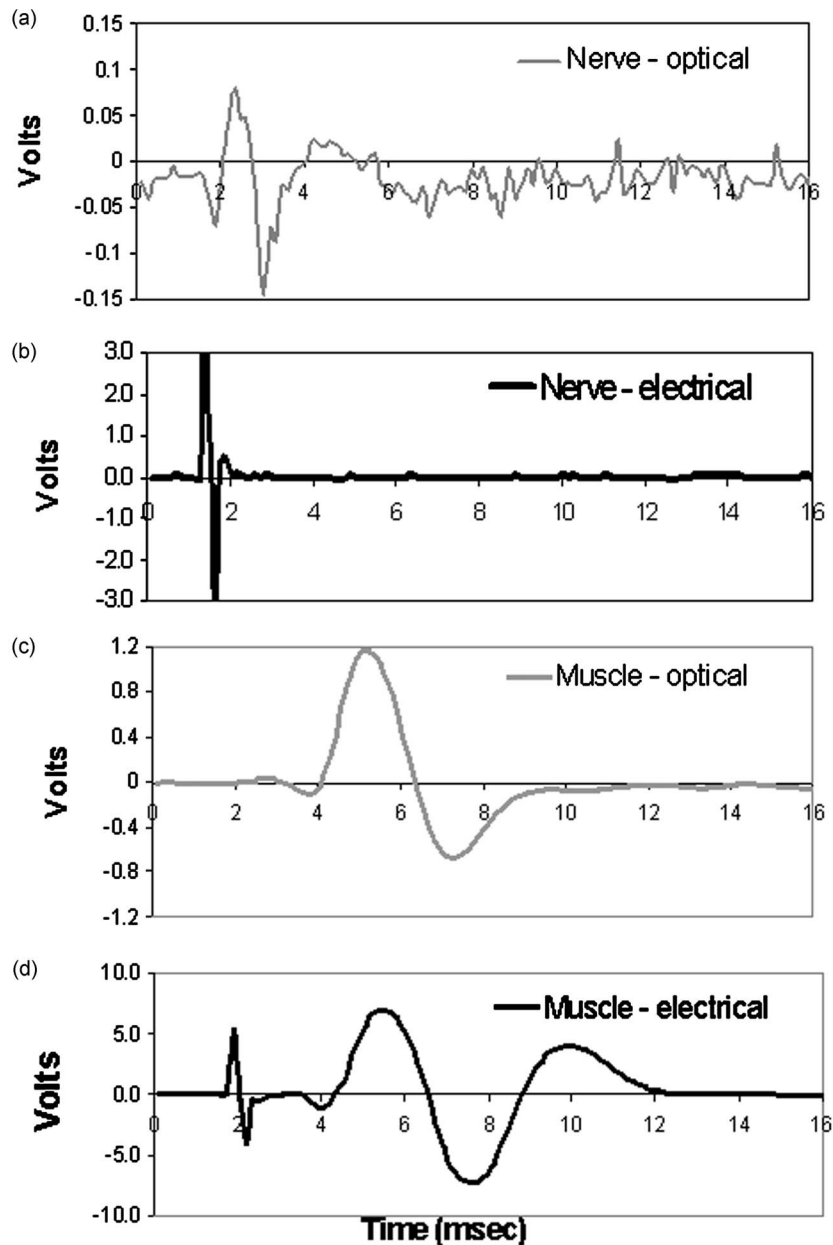
Fig. 2 Compound nerve and muscle action potentials recorded from sciatic nerve in rat. (a) CNAP recorded using optical stimulation at 2.12 μm, (b) CNAP from electrical stimulation, (c) hamstring CMAP recorded using optical stimulation at 2.12 μm, and (d) hamstring CMAP using electrical stimulation. The stimulation time for all recordings occurred at $t=0$ ms.

creased, a larger CNAP and CMAP amplitude response was seen. This relationship is similar to the strength-response curves observed from classical electrical stimulation experiments where the amplitude of the CNAP increased linearly with the magnitude of stimulation.[38]

Based on consistent observations of neuromuscular response to transient optical stimulus, experiments were performed *in vivo* in the rat model that verify ability of the incident light to produce a physiologically conducted AP within the nerve transmitted through a normal neuromuscular synaptic mechanism. A depolarizing neuromuscular blocker (succinylcholine) was applied to the muscle, resulting in preservation of the CNAP but loss of the CMAP. This confirmed that the potentials were being generated within the nerve and being propagated to the muscle through normal acetylcholine mediated synaptic transmission.

3.2 Wavelength Dependence and Safety for Optical Stimulation

In order to determine the optimal wavelength at which to induce action potential in peripheral motor neurons, a study was conducted to determine the wavelength dependence of the stimulation threshold. Figure 3(a) depicts both the stimulation and ablation thresholds as a function of wavelength for relative peaks and valleys in the spectral range from
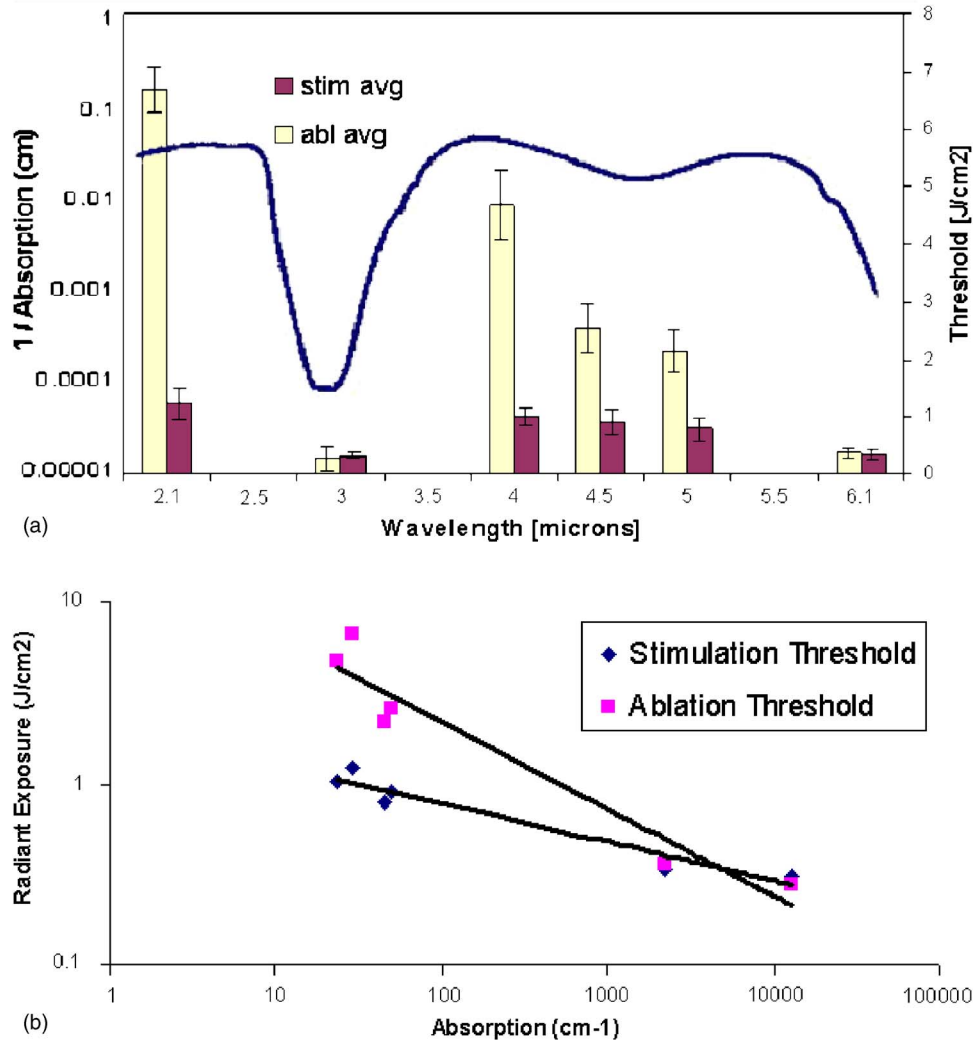
Fig. 3 (a) Wavelength dependence of stimulation. FEL employed to irradiate four different nerves for three trials each at six wavelengths, 2.1, 3.0, 4.0, 4.5, 5.0, and 6.1 μm, each near a relative peak or valley of water absorption (solid line). (b) Log-log plot of ablation and stimulation radiant exposure thresholds as a function of the water absorption coefficient for each wavelength.

2 to 6.1 μm. The most notable observations from this study are that these thresholds exhibit wavelength dependence, which approximates the inverse of the soft tissue absorption curve from FTIR spectrometer experiments [Fig. 3(a)], and tend to be less than ablation thresholds. The FTIR results are shown in the same graph (solid line) as the penetration depth spectrum (1/absorption) for nerve tissue. It is evident from the small standard deviations for all wavelengths studied (n =12) that these stimulation thresholds are fairly reproducible, similar to results from electrical stimulation.[39] Figure 3(b) illustrates general trends in the stimulation and ablation thresholds as a function of absorption coefficient using the data shown in Fig. 3(a). In both figures it can be observed that at high soft tissue absorption values the stimulation radiant exposure thresholds tend to be low (<1 J/cm^2). At valleys in soft tissue absorption, the opposite effect is observed, where the stimulation thresholds are higher (>1 J/cm^2). When observing the log-log plot of the stimulation and ablation radiant exposure threshold (H) as a function of wavelength and assuming that both processes are thermally induced, we would expect the relationship to be linear ($H=pc\Delta T/\mu_a$), since a power law can describe their relationship [Fig. 3(b)]. We see that at high absorption, the thresholds tend to be similar. At low tissue absorption, however, we notice a divergence in the ablation and stimulation thresholds. It is clear from this figure that the margin between damage and stimulation increases with decreasing tissue absorption. Based on these results, alternate suitable wavelengths may be inferred without measurement from nerve tissue absorption properties for maximum efficacy and minimum damage, such as $\lambda=2.1$ μm and 4 to 5 μm.

To determine the most appropriate and safest wavelengths for optical neural stimulation the results from Fig. 3 were used to obtain safety ratios at each wavelength, illustrated in Table 2. Large safety ratios are an excellent indicator for effective stimulation wavelengths that minimize tissue damage. The ratios for wavelengths 2.1, 3.0, 4.0, 4.5, 5.0, and 6.1 μm were experimentally determined using the FEL. These results indicate that the highest safety ratios are obtained at 2.1 (5.5) and 4.0 μm (5.0).

Table 2 Safety ratio shown for varying wavelength and the related penetration depth in sciatic nerve tissue obtained from FTIR spectroscopy measurements.

Laser	Ho:YAG	FEL	FEL	FEL	FEL	FEL	FEL
Wavelength (μm)	2.12	2.1	3.0	4.0	4.5	5.0	6.1
$1/\mu_{a,\text{nerve tissue}}$ (μm)	429.2	420.2	1.0	537.6	251.9	278.6	5.7
Safety ratio	6.25	5.50	0.88	4.61	2.76	2.73	1.07

Considering these promising results along with laser availability and the capability of fiber delivery at a wavelength of 2.1 μm, safety ratio experiments for 10 nerves were also measured using the holmium:YAG laser operating at $\lambda = 2.12$ μm. The average stimulation threshold radiant exposure for this laser and wavelength was 0.32 J/cm^2 with an average ablation threshold at 2.0 J/cm^2. Thus, the safety ratio with the holmium:YAG is over 6 (Table 2), designating this as a particularly enticing and convenient laser for optical nerve stimulation in a medical setting.

3.3 Histology of Optically Stimulated Peripheral Nerves

For this methodology to gain acceptance in basic laboratory study and perhaps even more importantly in clinical applications, it is important to show that no irreversible damage occurs when using optical stimulation for physiological purposes. Histological analysis was performed on excised nerves following acute stimulation to assess and quantify the damage accrued within the neural tissue with optical activation. The results from all samples analyzed, regardless of wavelength of stimulation, are shown in Table 3. Eight of the twelve irradiated nerves reveal no signs of thermal damage to the nerve fibers, three of which demonstrated slight reversible damage to the perineurium (grade 1). All samples that manifest grade 0 damage were irradiated at $\lambda = 4.0$ μm, which has the highest safety ratio amongst the wavelengths chosen for this study. Radiant exposures in these samples ranged from 0.13 to 0.243 J/cm^2, or up to 2 times threshold stimulation
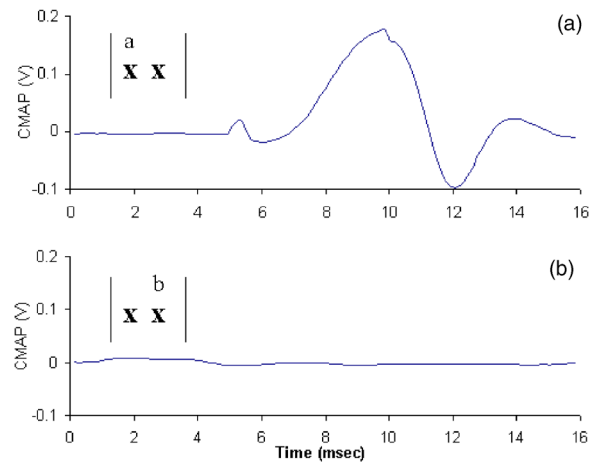
value. Each of the four wavelengths ($\lambda = 4.0$, 4.5, 5.0, and 5.5 μm) were represented in the grade 1 group, with radiant exposures averaging 2.4 times the experimentally derived stimulation threshold value (0.14 J/cm^2) determined in this set of experiments (see methods). The remaining four nerves were characterized as grade 3; all but one of these were stimulated using radiant exposures that were over 4 times the stimulation threshold value. Results excluding this erroneous data point are indicated in italics (Table 3). These histological findings suggest that nerves can be optically stimulated acutely without causing neural tissue damage, even when the radiant energy exposure is at least twice that of threshold AP generation.

3.4 Spatial Selectivity of Optical Stimulation

In addition to safety it is important to evaluate the efficacy of optical nerve stimulation in the peripheral nerve and validate the claim of improved spatial specificity using optical stimulation. To illustrate this concept, CMAP recordings were measured from a single muscle (the hamstring) as the optical fiber was translated across the sciatic nerve proximal to the first branch point (Fig. 4). Stimulation of the hamstring muscle only occurs when the laser spot is directly over the nerve

Table 3 Results from histological analysis from all samples irradiated with $\lambda = 4$, 4.4, 5, and 5.4 μm. The average fluence is shown for each grade (0 to 3) of thermal damage and this value is compared to the stimulation threshold. The grade 3 results in italics indicate the data set without the outlier in which the tissue was irradiated with 0.175 J/cm^2.

Severity of Damage	# Samples (n)	Avg. Fluence (J/cm^2)	X^* threshold
Grade 0	3	0.180±0.057	1.3
Grade 1	5	0.341±0.087	2.4
Grade 2	0		
Grade 3	4	0.424±0.190	3.0
		0.507±0.135	*3.6*

Fig. 4 Spatial selectivity of optical stimulation on the main sciatic nerve branch. (a) CMAP recorded in the hamstring muscle at position A corresponding to the fascicles innervating the hamstring. (b) CMAP recorded in the hamstring muscle at position B a distance of 300 μm from A, an adjacent fascicle within main sciatic nerve trunk proximal to the first branch point. The stimulation time for all recordings occurred at $t = 0$ ms.

fascicle innervating that muscle [Fig. 4(a)]. As the spot is moved to an adjacent fascicle on the trunk of the sciatic nerve, a CMAP is no longer recorded from the hamstring muscle [Fig. 4(b)]. In contrast, electrical stimulation of fascicle in the sciatic nerve leading to the hamstring muscle is nearly always accompanied with activation of other adjacent muscle fascicles due to the spread of electrical current beyond the electrode. Preliminary results clearly indicate the capability of optical stimulation to selectively target nerve fibers that innervate specific muscle groups by translation of the fiber probe across the main branch of the sciatic nerve.

4 Discussion

Optical stimulation is ideal for a number of procedures that routinely employ electrical stimulation in neurosurgery, such as intraoperative diagnostics. In peripheral nerve surgery, electrical stimulation is utilized to identify the connectivity and functionality of specific nerve roots to be avoided or resected,[40] although lack in spatial specificity places severe limitations on this technique. Neurostimulation of the spinal cord for pain relief has become another use for electrical stimulation treatment.[41] Cortical surface mapping of motor and sensory areas during brain tumor resection, or mapping deep brain structures for implantation of deep brain electrodes for stimulation, relies on electrical means to create a unique map of functional structures that varies among individuals.[41–43] Electrical deep brain stimulation (DBS) of small areas deep within the brain has become a novel, accepted technology in treatment of Parkinson's disease and other movement disorders that effectively substitutes the beneficial effects of drugs with that of electrical stimulation.[44] The spatial selectivity in determination of the most appropriate site for the stimulus lead may be enhanced though a noncontact optical stimulator, while a long-term optical device may one day replace the currently electrically implanted lead. There are a number of additional applications for electrical stimulation, many of which have not realized their full potential due to the inherent restrictions linked to existing stimulation techniques previously discussed. Here we provide the groundwork for advancement in technology with the innovation of optical stimulation of nerve tissue, which can be utilized to explore new applications for excitability of neural tissue hindered by the limitations of electrical stimulation.

The physiologic validity of the neural response from optical stimulation is evident when compared to the response obtained from electrical stimulation. Results indicate that the incident optical energy is directly responsible for the initiation of a normal AP resulting in propagation of the signal. The similarity in both the shape and timing of the graphs from Fig. 2 indicate that the time scales, thus conduction velocities, are similar for the two stimulation modalities, signifying that measured potentials are independent from the excitation mechanism. However, the stimulation artifact typically linked with traditional electrical stimulation-recording methods is not observed in the optically elicited nerve and muscle responses. For decades, the stimulation artifact associated with electrical stimulation has hindered electrophysiologists when attempting to stimulate and record within a confined volume of neural tissue, and interpretation of this signal is only possible for times after the artifact termination. The lack of

stimulation artifact in optically derived signals facilitates simultaneous stimulation and recording from adjacent portions of a neuron.

A linear relationship was observed between the optical radiant exposure and the strength of the recorded CNAP. This relationship was comparable to the strength-response curves observed with electrical stimulation. Generally, individual nerve fiber diameters and excitation thresholds vary by small increments. Although individual axons within the nerve bundle follow an all or none response to a stimulus, the CNAP reflects a population response to stimulation, and as more individual fibers are recruited by the stimulus, the observed response appears continuously graded. As the stimulus energy increases, more fibers are recruited resulting in the increased voltage recorded in the CNAP. Ultimately, as the maximum number of axons is recruited within the nerve, the response will reach a maximum voltage.

Electrical stimulation has an unconfined spread of charge leading to a graded response when stimulating excitable tissue.[45] In contrast, individual axons can be selectively stimulated to produce isolated, specific muscle contractions with optical excitation in a noncontact fashion, two major advantages associated solely with this modality. While it is possible to stimulate small areas or even individual cells using electrical stimulation, doing so requires physical insertion of the electrode in the target cell. This induces nerve damage through physical contact or membrane puncture and is thus inherently difficult or even impossible (i.e., single cell stimulation) *in vivo* due to constraints in electrode size compared to threshold current for activation.[46–48]

Preliminary data with optical nerve stimulation in mammals unequivocally confirms that optical nerve activation exhibits significant spatial specificity, or lack of spread of stimulus to neurons not in direct contact with the stimulus source. The precision and spatial specificity with optical excitation allows selective recruitment of nerve fibers as can be seen by comparing the relative magnitudes of nerve and muscle potentials (Fig. 2) elicited from optical and electrical stimulation. Note that electrically stimulated muscle recordings exhibit peak voltages of 7.5 V. On the other hand, optically evoked muscle recordings (1.15 V) demonstrate responses that are almost one order of magnitude lower than those found in electrical stimulation. This spatial precision can be attributed to both the ability to focus incident light and a smaller penetration depth from the optical stimulus as compared to the unconfined spread of charge from electrical stimulation. In turn, this leads to the recruitment of a smaller number of axons when using light, which is evidenced by the difference in magnitude of the responses. Comparison between these modalities demonstrates the spatial discrimination capability of optical excitation, whose precision is a function of the spot size and wavelength (i.e., penetration depth) used for stimulation. Thus, individual nerve fibers and muscles can be selectively stimulated for a controlled, explicit response within a peripheral nerve. In fact, for all optical stimulation experiments it was observed that a specific muscle or group of muscles contract depending on the location of the incident laser upon the nerve bundle (Fig. 4). Changing the position of the laser spot by a fraction of a millimeter yields a response from a different muscle group. This finding is in contrast to what is observed with electrical stimulation when done with a

hook electrode where each muscle innervated by the entire nerve bundle is stimulated resulting in a gross, uncoordinated twitch response from all innervated muscles.

The wavelength dependence of the optical stimulation thresholds yields pertinent wavelengths for the most favorable stimulation values based on the optical properties of the target neural tissue. Since absorption dominates scattering in the IR the hypothesis was that at wavelengths where absorption is least, light penetration depth (i.e., 1/absorption) is maximized, thus the nerve is more efficiently stimulated with less damage as photons are distributed over a greater tissue volume to minimize thermal injury. The ablation thresholds for nerve tissue, which is 80% water [as can be inferred from Fig. 3(a)], is inversely proportional to the water absorption curve. Note that the results from FTIR spectroscopy of neural tissue [shown as the inverse of absorption, Fig. 3(a)] are comparable to 80% of the values published for water absorption over the wavelengths of interest.[35] Results indicate that the radiant exposure required to stimulate is lower at wavelengths with high absorption (i.e., easier to stimulate) and higher at wavelengths with low absorption. However, it is also easier to ablate at wavelengths with high absorption. Thus, a more effective representation of optimal stimulation wavelengths is the safety ratio. It can be observed from results depicted in Table 2 that this safety ratio also follows tissue penetration depth as a function of wavelength, indicating that the safety ratio is largest at wavelengths where the radiant exposures for stimulation are much lower than those required for ablation. The highest safety ratios are obtained at 2.1 and 4.0 μm, which correspond to valleys in water absorption and equivalent absorption coefficients. There are few lasers that exist at 4.0 μm in wavelength, however, the holmium:YAG laser at 2.12 μm is commercially available and is currently used for many clinical applications. Furthermore, light can be delivered via a fiber optic at this wavelength, enhancing the clinical attractiveness of this laser. In fact, it is reasonable to assume that any wavelength yielding a penetration depth between 300 and 500 microns will be an optimal wavelength for stimulation based on the tissue geometry of a peripheral nerve. By matching the absorption values of the wavelengths yielding the highest safety ratio with commercially available pulsed lasers, a clinically useful benchtop laser becomes a possibility.

The ability to tune the FEL allowed the exploration of the IR spectrum for determination and assessment of the optimal stimulation wavelength, hence generating insight into the most appropriate laser for clinical applications. We infer from these results that clinically relevant wavelengths will not occur at peaks in soft tissue absorption because the safety ratio for these absorption values is low, or energy required to produce action potentials within the nerve is roughly equal to the energy for ablation. For example, the penetration depth at $\lambda = 3$ μm is roughly 1 μm in soft tissue (Table 2). In this case, only through thermal diffusion or pressure wave propagation (depending on the underlying mechanism) does the heat or photon energy reach the neural fibers. Overall, roughly 100 to 200 μm of connective tissue lies between the nerve surface and the first layer of axons.[49] By the time the energy reaches the axonal fibers, ablation of the epineurium has already occurred. We can also predict that absolute valleys in the water absorption curve (i.e., visible, UV, and NIR region,

300 to 1800 nm) will not yield optimal wavelengths, because the low absorption will distribute the light through a large depth leading to insufficient energy delivered to the nerve fibers for an elicited response. This suspicion was confirmed in stimulation experiments when a pulsed alexandrite laser ($\lambda = 755$ nm), where tissue absorption is very low, resulted in no stimulation effect upon irradiation (unpublished data). Thus, the most promising wavelengths in this study were found to occur in the infrared at 2.12 and 4 to 5 μm, which fall in the intermediate range of water or soft tissue absorption characteristics. Volumetric heating as well as spatial recruitment need to be considered when selecting the most appropriate wavelength for optical stimulation. Optimal wavelengths are those in which the volume of heating and therefore the penetration of photons is deep enough to prevent surface ablation and that these photons propagate through the outer sheath of the epineurium to reach the actual axons where action potentials are generated. From these results it is clear that the most appropriate wavelengths for selective stimulation of peripheral nerves with presently available lasers occurs at relative valleys in the IR absorption region of soft tissue, such as the holmium:YAG laser wavelength at 2.12 μm. More importantly, the depth of penetration, and therefore the selectivity in depth of neuronal fiber recruitment within a nerve, can be tailored based solely on the IR wavelength applied. Also the spotsize can easily be adjusted for precision in three dimensions.

Undoubtedly, the microstructure of myelin and connective tissues overlying neural axons is unique compared to the bulk properties of the nerve tissue used in many of our assumptions. While the microstructure of the tightly packed lipids comprising myelin sheaths presents a morphologically distinct layer of tissue, our results from FTIR measurements of nerve tissue and stimulation threshold wavelength dependence clearly show that this phenomenon follows the water or soft tissue absorption curve. At 2.1 μm (4600 cm^{-1}) there are no selective absorption bands for lipids and cholesterol, the main constituents of myelin.[50] All bands of lipids occur between 1000 and 1600 cm^{-1} and bands of cholesterol in the IR occur at 5.75 μm.[51] Therefore we have no reason to suspect that myelin will selectively absorb additional light than that predicted from the bulk absorption properties of nerve tissue reported in this paper.

In most therapeutic laser applications, laser-tissue interaction is mediated by a thermal or thermomechanical process that depends on the operational parameters of the laser, such as wavelength (λ), pulse duration (τ), and laser radiant exposure or irradiance [i.e., the energy/area (J/cm^2) or power/area (W/cm^2)]. Experiments described here clearly define the most efficient wavelength(s) for optimal stimulation of the peripheral nerve and suggest a range of radiant exposures for safe excitation without causing tissue damage; however, study of additional laser parameters is still needed to distinctly characterize the most suitable instrumentation for optical neural activation in clinical situations. From these studies reported here, we see that the stimulation threshold with the FEL ($\tau = 5$ μs) at 2.1 μm is roughly 1.25 J/cm^2, whereas the threshold for excitation with the Ho:YAG laser ($\tau = 350$ μs) at this same wavelength is 0.32 J/cm^2. These results suggest that a longer pulse leads to lower threshold stimulation, although the

efficiency in stimulation associated with these two lasers is roughly the same as evidenced by their similar safety ratios (Fig. 4). Consequently, initial results indicate that the pulse duration is not a significant factor in the design of an optimal neural stimulation device, but further study of the safety ratio as a function of the stimulus duration is needed to confirm this suspicion.

For the optimal laser parameters used in this study, it is essential to define an exact range of "safe" laser radiant exposures, or the values between threshold and the upper end of radiant exposures that do not result in functional tissue damage, to facilitate defining what is appropriate for clinical use. Initial results indicate that this upper limit will be about 2.5 times the energies required for stimulation. Another key parameter for efficient laser stimulation is the repetition rate. As the repetition rate increases, the heat load to the tissue will increase accordingly. Most significantly, we expect that as the time between pulses decreases, there will be less time for heat diffusion, eventually resulting in more significant heat buildup. We anticipate that increasing the repetition rate will lower the threshold for damage. However, it is also conceivable that the increased thermal accumulation in the target tissue may lower the stimulation threshold, thus partially offsetting the decrease in safety margin owing to thermal superposition that may occur with additional laser pulses. Future studies are needed to resolve the relative importance of each of the laser parameters and to determine optimal combinations that facilitate higher frequency stimulation.

Histological analysis reveals promising results in that 8 of 12 stimulated nerves show no signs of thermal damage at energies up to 2.5 times the threshold value, indicating the potential for this stimulation modality. It should be noted that all four grade 2 or 3, or damaged nerves, were irradiated with energies at least 4 times stimulation threshold radiant exposure with the exception of one nerve irradiated near threshold with 0.175 J/cm^2. While the reason for this single outlier is unknown, the damage seen here may be a result of mishandling of the nerve during the procedure and not a direct result of laser stimulation. To address this concern, acute and survival experiments, with a sham procedure performed in the contralateral leg for true control in which sham nerves are exposed and handled similar to irradiated nerves, need to be performed to control for these effects. Several experimental nerves demonstrated thermal coagulation lesions in the perineurium and slight thermal damage in the subjacent nerve. These findings suggest that 3- to 5-day survival studies should be performed to note the extent of lethal damage, if any, by tissue necrosis and Wallerian degeneration of the distal axons. Future studies conducted at 2.12 μm, a "safer" wavelength than 4 μm, will be conducted to identify the maximum threshold value at which optical stimulation produces no visible thermal changes and no damage to the nerve tissue.

The stimulation threshold was much lower in the histology experiments than can be seen in Fig. 3(a). This reduced threshold can be explained with respect to the thickness of the nerve bundle casing of the main peripheral nerve trunk used for safety ratio experiments containing numerous motor branches, compared to the smaller fascicles containing only the axons innervating a specific muscle stimulated for histological analysis. With larger nerve trucks the epineurial layer

is much thicker than in individual fascicles or smaller nerves surrounded by a thinner perineural layer. Thus, more laser energy is needed to reach the underlying axons and therefore for generation of an action potential. Additionally, the propensity of individual axons and fascicles to undergo a variety of twists and turns within the nerve bundle could explain the sample-to-sample variation in threshold seen in Fig. 3(a). For example, the lowest threshold (smallest) fascicles innervating a particular muscle may be close to the nerve surface and just below the epineurial layer. Similarly, larger threshold radiant exposures may result from larger fascicles lying well below the surface of the nerve (200 to 300 μm). Additional studies need to be conducted in various size nerves to determine these threshold differences. Nonetheless, results demonstrate a safe range of radiant exposure up to 2.5 times the stimulation threshold.

Optical stimulation has been shown to be an effective method for stimulation of nerve cells, but the mechanism for this effect is unknown to date. In order to apply this technology in human applications, it is important to understand the mechanism of optical stimulation of neural tissue. Light interacts with the neural tissue through a process of absorption and scattering of photons providing a free energy transition, which results in a photobiological effect on the tissue producing an action potential. The use of lasers in medical procedures can be grouped into two distinct categories, therapeutic and diagnostic/imaging applications. For therapeutic procedures, for instance optical stimulation, the interaction between the laser and biological tissue can be separated into, at least, three mechanistic categories, (1) photochemical, (2) photothermal, and (3) photomechanical (for review see Ref. 37). Photobiological effects of laser tissue interaction can be separated into three distinct categories; photochemical, photothermal, and photomechanical effects.[52] Photothermal effects result from the transformation of absorbed light energy to heat and an associated temperature change within the tissue, which may lead to destruction of the target tissue. This transfer of energy from photon energy to heat may be one possibility for the underlying origin for stimulation to occur. In fact, it is well known that increase in temperature can change both the conductance of sodium and calcium channels in neurons, each responsible for membrane depolarization, and the transmembrane potential of any cell.[53–56] Photomechanical effects are secondary effects due to rapid heating with very short laser pulses, which produce a mechanical force in the form of a transient pressure wave that propagates to superficial layers of irradiated tissue. Theoretically, thermoelastic pressure waves produced as a result of heat produced from photon energy may occur. This propagating pressure wave may activate various ion channels sensitive to stretch, mimicking mechanical stimulation of the nerve fibers. While it is possible that pulsed laser irradiation induces pressure waves in the target tissue owing to the thermoelastic effect, the contributions of this to optical stimulation are expected to be minimal with the laser parameters used; the pulse duration exceeds the stress confinement time for this wavelength by nearly 3 orders of magnitude resulting in a dissipation of thermally induced expansion during the laser pulse and consequently little pressure buildup.[57,58] Moreover, the radiant exposures needed for optical stimulation are such that even if stress buildup was facilitated, as would be the case for much shorter laser pulses, the

theoretical maximum pressure increase is only on the order of 10 bar. Photochemical effects are attributed to the changes in chemical composition of the tissue from photon energy. No one to date has published the photosensitive properties of peripheral neurons at the chemical level. Thus, at present we hypothesize this photobiological interaction (i.e., laser energy leading to neuronal stimulation) to be a combined thermomechanical effect within the nerve tissue. We further propose that the relative contributions from the thermal and mechanical stimulatory mechanisms are dependent on the wavelength used in excitation. Future experiments designed to examine the exact nature of this laser-nerve tissue interaction will reveal the fundamental mechanism of excitation.

Thus, we have described a new modality for efficient, artifact-free stimulation of neurons using pulsed, low-energy laser light at radiant exposures well below tissue damage thresholds. This modality has the potential to change the future of electrophysiology in the laboratory as well as the clinical setting. The spatial selectivity of optical stimulation presents an opportunity for detailed mapping and repair of peripheral nerves, while artifact-free signals promote adjacent stimulation and recording from the same nerve or neuron. The opportunity to map neural function with higher spatial precision than is currently in practice is presented. Other benefits include contact free stimulation, which reduces the likelihood of physical damage due to mechanical contact with electrodes. At the present time, a commercially manufactured, portable laser operating at an optimal wavelength determined from this study has been shown to be an effective method for eliciting nerve and muscle potentials. The ability to couple this optimal wavelength through fiber optics helps to significantly reduce the invasiveness for numerous neurosurgical procedures that utilize nerve stimulation. With the emergence of compact and economical laser diodes and chip lasers, the construction of a self-contained, handheld device for optical stimulation of nerves during clinical procedures and even an implantable device for future therapies may soon become a reality.

Acknowledgments

References

1. G. a. H. Fritsch and E. Hitzig, "Ueber die elektrische Erregbarkeit der Grosshirns," *Archiv Anatomie, Physiologie und Wissenchaftlische Medicin* **37**, 300–332 (1870) (in German).
2. L. A. Geddes, *Electrodes and the Measurement of Bioelectric Events*, Wiley-Interscience, New York (1972).
3. O. Devinsky, "Electrical and magnetic stimulation of the central nervous system. Historical overview," *Adv. Neurol.* **63**, 1–16 (1993).
4. R. H. Pudenz, "Neural stimulation: clinical and laboratory experiences," *Surg. Neurol.* **39**(3), 235–242 (1993).
5. J. K. Song, B. Abou-Khalil, and P. E. Konrad, "Intraventricular monitoring for temporal lobe epilepsy: report on technique and initial results in eight patients," *J. Neurol., Neurosurg. Psychiatry* **74**(5), 561–565 (2003).
6. J. Vaquero, M. Manrique, S. Oya, and G. Bravo, "Tissue damage after chronic cerebellar stimulation," *Acta Neurochir.* **56**(3–4), 860–862 (1981).
7. M. Zuccarello et al., "Spontaneous cerebellar hematoma associated with chronic cerebellar stimulation. Case report," *J. Neurosurg.* **65**(6), 860–862 (1986).
8. S. N. Baker et al., "Multiple single unit recording in the cortex of monkeys using independently moveable microelectrodes," *J. Neurosci. Methods* **94**(1), 5–17 (1999).
9. L. A. Geddes and J. D. Bourland, "Tissue stimulation: theoretical considerations and practical applications," *Med. Biol. Eng. Comput.* **23**(2), 131–137 (1985).
10. K. McGill, K. L. Cummins, L. J. Dorfman, B. B. Berlizot, K. Leutkemeyer, D. G. Nishimura, and B. Wiidrow, "On the nature and elimination of stimulus artifact in nerve signals evoked and recorded using surface electrodes," *IEEE Trans. Biomed. Eng.* **29**(2), 129–137 (1982).
11. C. A. Miller, P. J. Abbas, and C. J. Brown, "An improved method of reducing stimulus artifact in the electrically evoked whole-nerve potential," *Ear Hear.* **21**(4), 280–290 (2000).
12. J. Booth, A. von Muralt, and R. Stampfli, "The photochemical action of ultra-violet light on isolated single nerve fibres," *Helv. Physiol. Pharmacol. Acta* **8**(2), 110–127 (1950).
13. R. Orchardson, "The generation of nerve impulses in mammalian axons by changing the concentrations of the normal constituents of extracellular fluid," *J. Physiol. (London)* **275**, 177–189 (1978).
14. G. Cruccu and A. Romaniello, "Jaw-opening reflex after CO_2 laser stimulation of the perioral region in man," *Exp. Brain Res.* **118**(4), 564–568 (1998).
15. D. Bragard, A. C. Chen, and L. Plaghki, "Direct isolation of ultra-late (C-fibre) evoked brain potentials by CO_2 laser stimulation of tiny cutaneous surface areas in man," *Neurosci. Lett.* **209**(2), 81–84 (1996).
16. J. B. Walker and L. K. Akhanjee, "Laser-induced somatosensory evoked potentials: evidence of photosensitivity in peripheral nerves," *Brain Res.* **344**(2), 281–285 (1985).
17. J. Walker, "Relief from chronic pain by low laser irradiation," *Neurosci. Lett.* **43**, 339–344 (1983).
18. W. H. Wu et al., "Failure to confirm report of light-evoked response of peripheral nerve to low power helium-neon laser light stimulus," *Brain Res.* **401**(2), 407–408 (1987).
19. P. Balaban et al., "He-Ne laser irradiation of single identified neurons," *Lasers Surg. Med.* **12**(3), 329–337 (1992).
20. R. L. Fork, "Laser stimulation of nerve cells in Aplysia," *Science* **171**(974), 907–908 (1971).
21. K. A. Horvath et al., "Transmyocardial laser revascularization: results of a multicenter trial with transmyocardial laser revascularization used as sole therapy for end-stage coronary artery disease," *J. Thorac. Cardiovasc. Surg.* **113**(4), 645–653 (1997).
22. G. Allegre, S. Avrillier, and D. Albe-Fessard, "Stimulation in the rat of a nerve fiber bundle by a short UV pulse from an excimer laser," *Neurosci. Lett.* **180**(2), 261–264 (1994).
23. H. Hirase et al., "Multiphoton stimulation of neurons," *J. Neurobiol.* **51**(3), 237–247 (2002).
24. J. D. Wells, C. Kao, K. Mariappan, J. Albea, E. D. Jansen, P. Konrad, and A. Mahadevan-Jansen, "Optical stimulation of neural tissue *in vivo*," *Opt. Lett.* **30**(5), 504–507 (2005).
25. C. Chiu, H. H. Chan, W. S. Ho, C. K. Yeung, and J. S. Nelson, "Prospective study of pulsed dye laser in conjunction with cryogen spray cooling for treatment of port wine stains in Chinese patients," *Dermatol. Surg.* **29**(9), 909–915 (2003).
26. N. Wu, E. D. Jansen, and J. M. Davidson, "Comparison of mouse matrix metalloproteinase 13 expression in free-electron laser and scalpel incisions during wound healing," *J. Invest. Dermatol.* **121**(4), 926–932 (2003).
27. N. Kanjani et al., "Wavefront- and topography-guided ablation in myopic eyes using Zyoptix," *J. Cataract Refractive Surg.* **30**(2), 398–402 (2004).
28. R. Puls et al., "Double contrast MRI of thermally ablated liver metastases," *Rofo Fortschr Geb Rontgenstr Neuen Bildgeb Verfahr* **175**(11), 1467–1470 (2003).
29. L. W. Knott, J. Katz, and L. J. Rubinstein, "Separate and combined effects of phenol, hyaluronidase and dimethyl sulfoxide on the sciatic nerve of the rat. I. Acute studies," *Arch. Phys. Med. Rehabil.* **49**(2), 100–104 (1968).
30. A. D. Izzo et al., "*In vivo* optical imaging of expression of vascular endothelial growth factor following laser incision in skin," *Lasers Surg. Med.* **29**(4), 343–350 (2001).
31. G. Edwards et al., "Tissue ablation by a free-electron laser tuned to the amide II band," *Nature* **371**(6496), 416–419 (1994).
32. G. S. Edwards and M. S. Hutson, "Advantage of the Mark-III FEL

for biophysical research and biomedical applications," *J. Synchrotron Radiat.* **10**(5), 354–357 (2003).

33. M. A. Mackanos et al., "Delivery of midinfrared (6 to 7-microm) laser radiation in a liquid environment using infrared-transmitting optical fibers," *J. Biomed. Opt.* **8**(4), 583–593 (2003).

34. H. S. Pratisto, S. R. Uhlhorn, and E. D. Jansen, "Beam delivery of the Vanderbilt free electron laser with hollow wave guides: Effect on temporal and spatial pulse propagation," *Fiber Integr. Opt.* **20**(1), 83–94 (2001).

35. A. J. Welch and M. J. C. v. Gemert, "Optical-thermal response of laser-irradiated tissue," in *Lasers, Photonics, and Electro-optics*, Plenum Press, New York (1995).

36. S. Thomsen, "Identification of lethal injury at the time of photothermal treatment," in *Laser-Induced Interstitial Thermotherapy*, SPIE Press, Bellingham, WA (1995).

37. S. Thomsen, "Pathologic analysis of photothermal and photomechanical effects of laser-tissue interactions," *Photochem. Photobiol.* **53**(6), 825–835 (1991).

38. L. A. Geddes and J. D. Bourland, "The strength-duration curve," *IEEE Trans. Biomed. Eng.* **32**(6), 458–459 (1985).

39. V. B. Mountcastle, *Medical Physiology*, 13th ed., Mosby, Saint Louis, MO (1974).

40. H. Ueno et al., "Endoscopic carpal tunnel release and nerve conduction studies," *Int. Orthop.* **24**(6), 361–363 (2001).

41. R. L. Weiner, "Peripheral nerve neurostimulation," *Neurosurg. Clin. N. Am.* **14**(3), 401–408 (2003).

42. F. E. Roux and M. Tremoulet, "Organization of language areas in bilingual patients: a cortical stimulation study," *J. Neurosurg.* **97**(4), 857–864 (2002).

43. P. A. Starr et al., "Implantation of deep brain stimulators into the subthalamic nucleus: technical approach and magnetic resonance imaging-verified lead locations," *J. Neurosurg.* **97**(2), 370–387 (2002).

44. A. L. Benabid et al., "Long-term electrical inhibition of deep brain targets in movement disorders," *Mov Disord.* **13**, Suppl. 3, 119–125 (1998).

45. T. F. Weiss, *Cellular Biophysics*, MIT Press, Cambridge, Mass. (1996).

46. H. Asanuma, A. Arnold, and P. Zarzecki, "Further study on the excitation of pyramidal tract cells by intracortical microstimulation," *Exp. Brain Res.* **26**(5), 443–461 (1976).

47. S. D. Stoney Jr., W. D. Thompson, and H. Asanuma, "Excitation of pyramidal tract cells by intracortical microstimulation: effective extent of stimulating current," *J. Neurophysiol.* **31**(5), 659–669 (1968).

48. J. B. Ranck Jr., "Which elements are excited in electrical stimulation of mammalian central nervous system: a review," *Brain Res.* **98**(3), 417–440 (1975).

49. E. R. Kandel, J. H. Schwartz, and T. M. Jessell, *Principles of Neural Science*, 4th ed., McGraw-Hill, New York (2000).

50. L. A. Horrocks, "Composition of myelin from peripheral and central nervous systems of the squirrel monkey," *J. Lipid Res.* **8**(6), 569–576 (1967).

51. Y. Fukami and K. Awazu, "The thermal dissociation of cholesterol esters using a 5.75 micron-free electron laser," *Proc. SPIE* **4961**, 106–113 (2003).

52. S. L. Jacques, "Laser-tissue interactions. Photochemical, photothermal, and photomechanical," *Surg. Clin. North Am.* **72**(3), 531–558 (1992).

53. J. R. Schwarz, "The effect of temperature on Na currents in rat myelinated nerve fibres," *Pfluegers Arch.* **406**(4), 397–404 (1986).

54. P. Jonas, "Temperature dependence of gating current in myelinated nerve fibers," *J. Membr. Biol.* **112**(3), 277–289 (1989).

55. E. van Lunteren, K. S. Elmslie, and S. W. Jones, "Effects of temperature on calcium current of bullfrog sympathetic neurons," *J. Physiol. (London)* **466**, 81–93 (1993).

56. R. Wondergem and L. B. Castillo, "Effect of temperature on transmembrane potential of mouse liver cells," *Am. J. Physiol.* **251**(4) (Pt. 1), C603–613 (1986).

57. A. J. Welch et al., "Laser thermal ablation," *Photochem. Photobiol.* **53**(6), 815–823 (1991).

58. E. D. Jansen et al., "Effect of pulse duration on bubble formation and laser-induced pressure waves during holmium laser ablation," *Lasers Surg. Med.* **18**(3), 278–293 (1996).